

**Zener tunneling in superlattices in a magnetic field**

D. Meinhold and K. Leo

*Technische Universität Dresden, Institut für Angewandte Photophysik, 01062 Dresden, Germany*

N. A. Fromer and D. S. Chemla

*Department of Physics, University of California at Berkeley, Berkeley, California 94720  
and Materials Sciences Division, E. O. Lawrence Berkeley National Laboratory, Berkeley, California 94720*

S. Glutsch and F. Bechstedt

*Friedrich-Schiller-Universität Jena, Institut für Festkörpertheorie und Theoretische Optik, Max-Wien-Platz 1, 07743 Jena, Germany*

K. Köhler

*Fraunhofer-Institut für Angewandte Festkörperphysik, 79108 Freiburg, Germany*

(Received 15 October 2001; revised manuscript received 14 January 2002; published 15 April 2002)

We present a study of the Zener effect in the optical absorption of strongly coupled superlattices with both a magnetic and an electric field in growth direction. The in-plane continuum of electron states is discretized due to Landau quantization, which allows to directly observe the transition from discrete to continuum states due to Zener tunneling in a true 1D system.

DOI: 10.1103/PhysRevB.65.161307

PACS number(s): 78.20.Jq, 71.35.Ji, 78.66.Fd

Superlattices are artificial semiconductors where the periodic modulation of conduction and valence band in one spatial direction (usually chosen as the  $z$  direction) leads to periodic potentials for the electrons and holes, similar to Bloch electrons in natural crystals.<sup>1</sup> In contrast to natural crystals, properties like the potential depth and the coupling between the wells can be adjusted by growth and material parameters. Furthermore, the time, space, and energy scales of superlattice excitations are mesoscopic making many phenomena (that would require extreme conditions in crystals) readily accessible to experiments in these heterostructures. Superlattices are thus ideal model systems to study the basic electronic and transport properties of periodic potentials. For instance, if an electric field is applied parallel to the growth axis, Wannier-Stark ladders<sup>2,3</sup> and its pendant, Bloch oscillations,<sup>4</sup> are observed in linear and nonlinear optical experiments. However, superlattice are not true 1D systems. Since their elementary excitations exhibit to dispersion in  $x$  and  $y$  direction they behave as quasi-3D systems.

The fact that the spectrum of a Bloch electron in an electric field consists of equally spaced energy levels has been predicted decades ago.<sup>5,6</sup> This was followed, however, by a long controversy on the nature of the spectrum, discrete resonances vs entirely continuous, when the coupling to higher bands is accounted for.<sup>7</sup> It has been shown analytically that the spectrum is continuous,<sup>8</sup> but shows equally spaced resonances in the density of states. This is confirmed by numerical calculations, based upon discretization of the Schrödinger operator in real space, which reveal a continuous density of states and eigenfunctions with an infinite extension.<sup>9,10</sup>

In contrast to the extensive theoretical studies, there has only been limited experimental investigations. The Wannier-Stark ladder has been studied for quasi-3D case superlattices (Refs. 2,3 and others) on samples with rather deep wells and weak coupling, so that the coupling to higher bands was negligible. In these experiments, the Wannier-Stark ladder

was present for low electric fields; for higher fields, the wave function began to localize within one well and the ladder disappears from the optical spectrum. For samples with strong coupling, neither the electronic spectrum nor the transport properties have been explored experimentally. This is surprising since the coupling to higher bands leads to Zener tunneling predicted long ago.<sup>11</sup>

Recently, we have presented studies of the continuous nature of the spectrum in strongly coupled shallow superlattices, where only the first miniband is within the potential wells.<sup>12,13</sup> Here, the transition from the discrete to the continuous spectrum with increasing electric field is accompanied by a drastic increase of the spatial extension of the eigenfunctions. This delocalization effect can be interpreted as Zener tunneling between discrete resonances from below-barrier states and the continuum of above-barrier states. We have observed that the increase of the transition line broadening directly follows the predictions for the tunneling rate in Zener's original paper.<sup>11</sup> Unfortunately, the effect is somehow masked by Fano interference that appears owing to the coupling between the discrete exciton resonance and the in-plane  $x$ - $y$  continuum of energetically lower Wannier-Stark transitions, and extensive theory is necessary to distinguish between the two broadening mechanisms.

In this Rapid Communication we present the experimental evidence for the Zener effect in a true 1D system: a superlattice in a magnetic field parallel to the  $z$  direction. Hereby, the Landau quantization produces discrete energy eigenvalues for the motion in the  $x$ - $y$  plane and removes the associated continuum. If Zener tunneling plays a major role, a discrete resonance will turn into a continuum of states as the electric field increases and the continuous spectrum were to have its origin in the electron motion along the  $z$  direction only. If, on the other hand, the picture of discrete Wannier-Stark ladders were to remain true, for any finite electric field  $F$  the optical spectrum should entirely consist of discrete transition lines.

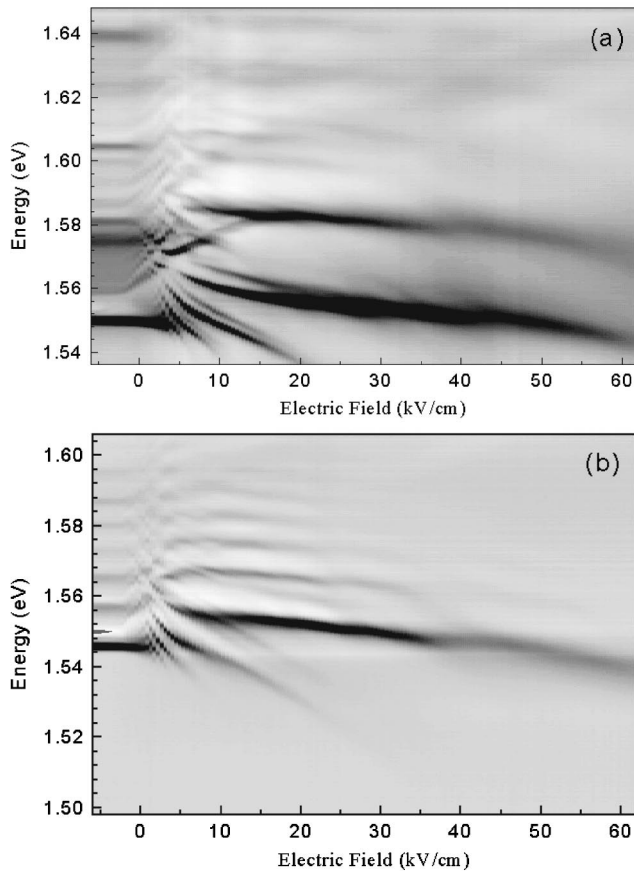


FIG. 1. Gray-scale plots of the absorption as a function of applied electric field. (a)  $B = 10$  T;  $\sigma^+$  polarization. (b)  $B = 4$  T;  $\sigma^-$  polarization.

As in Refs. 12,13, we used a 35 period 76/39 Å GaAs/ $\text{Al}_{0.08}\text{Ga}_{0.92}\text{As}$  shallow superlattice, grown by molecular-beam epitaxy. The sample was designed so that there is only one below-barrier electron miniband<sup>14</sup> having a band width of 28 meV. The barrier height for the electron is 63.2 meV. The lower and upper edges of the first miniband, relative to the GaAs conduction-band edge are 19.1 meV and 35.2 meV, respectively. The gap between first (below barrier) and second (above barrier) miniband is 33.3 meV.

With the effective electron mass of  $m_e = 0.067m_0$  and the in-plane cyclotron masses for heavy hole (hh) and light hole (lh),  $m_{\text{hhc}} = 0.491m_0$  and  $m_{\text{lhc}} = 0.0857m_0$ , respectively,<sup>15</sup> the cyclotron energy for the hh and lh transition is about  $1.96 \text{ meV} \times B/\text{Tesla}$  and  $3.08 \text{ meV} \times B/\text{Tesla}$ , respectively. These energies are not directly observed due to hole mixing and interference between Wannier-Stark and Landau quantization.

The superlattice is embedded in several buffer layers with high lateral conductivity to ensure both homogeneity and constancy of the electric field over all wells. The GaAs substrate was partially removed by selective wet etching to allow for optical transmission measurements. A reverse-bias dc-voltage was applied via an Ohmic and a semi-transparent Schottky contact.

The sample was held at liquid Helium temperature in a split-coil magnet, and magnetic fields up to 10 Tesla were

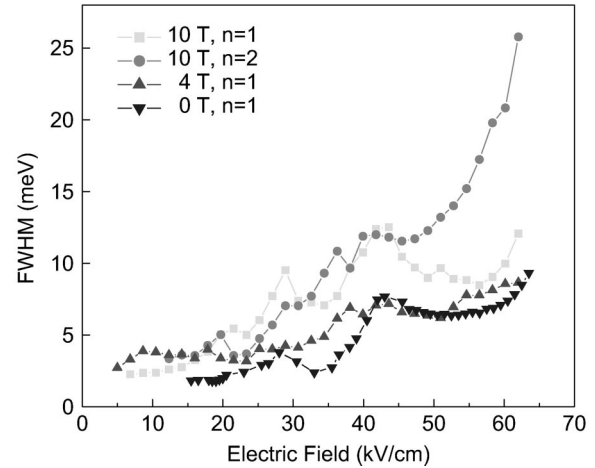


FIG. 2. Line width (FWHM) of the diagonal transition for  $B = 0, 4,$  and  $10$  T as a function of electric field.

applied in the  $z$  direction. The linear absorption measurements were performed in transmission geometry using a halogen lamp as continuum source. The transmitted beam was spectrally resolved in an optical multichannel analyzer comprising a monochromator and a CCD camera. The transmission spectra were corrected for the spectrum of the light source and Fabry-Perot interferences within the sample. The internal electric field  $F$  was calibrated using the splitting of the Wannier-Stark levels at magnetic field  $B = 0$  T.

In the absence of a magnetic field we observed a good quantitative agreement between theory and experiment.<sup>13</sup> Although magneto-exciton spectra are more sensitive to details of the band structure such as nonparabolicity, mass reversal, and hole mixing, theory and experiment should have qualitatively the same behavior when the magnetic field is present. Although the main results are readily understood by direct inspection of the experimental data, we also present a comparison with a two-band model, with and without Zener tunneling, based on the theoretical approach of Ref. 13.

Figure 1 gives an overview over the excitonic transitions in the presence of an electric and magnetic field. The optical absorption as function of the photon energy and the electric field is shown as a gray-scale plot for fixed magnetic fields  $B = 10$  T (a) and  $B = 6$  T (b). A plot for zero magnetic field can be found in Ref. 12. One can clearly see the Wannier-Stark ladders associated with the first ( $n = 0$ ) and second ( $n = 1$ ) Landau level. Furthermore, the spectrum in Fig. 1(a), which is taken with  $\sigma^+$  polarization, shows a Zeeman splitting.<sup>16</sup> This feature is absent in Fig. 1(b), which is taken with  $\sigma^-$  polarization. We also notice an increase of the line broadening with increasing electric field, which is a signature of Zener tunneling.

The line width [full width at half maximum (FWHM)] for the first and second Landau level as function of the electric field is shown in Fig. 2. The line width shows an overall increase with electric field for all values of the magnetic field. For  $F = 60$  kV/cm, the line width of the second Landau level at 10 T has increased by a factor of ten, compared to  $F = 0$ . We also observe strong resonances in all curves at about  $F = 28$  kV/cm and  $F = 43$  kV/cm, which is due to

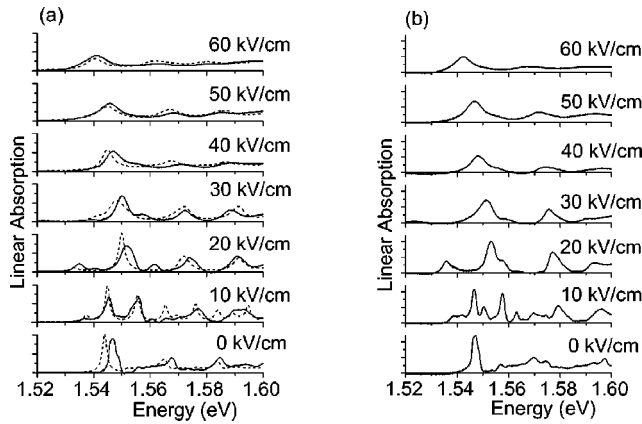


FIG. 3. Absorption spectra for  $B=9$  T and  $F=0, \dots, 60$  kV/cm. (a)  $\sigma^-$  polarization. (b)  $\sigma^+$  polarization. Experiment: solid line, theory: dashed line.

anticrossings with other Wannier-Stark ladders.

In the following, the underlying physics is discussed on exemplary spectra in detail: experimental spectra obtained for a magnetic field of  $B=9$  T are shown in Fig. 3 for left-circular (a) and right-circular (b) polarization and for electric fields  $F=0, \dots, 60$  kV/cm. For comparison, the results of a numerical calculation are shown by the dashed lines. For  $F=0$ , the lowest resonance is an isolated peak with a small homogeneous broadening. The departure from the Lorentzian form results from the degeneracy between heavy- and light-hole transitions. In the  $\sigma^-$  spectrum it can be seen that indeed the lowest peak actually consists of two closely spaced lines. Still at  $F=0$  the higher resonances are broadened by Fano interference with lower Landau level  $z$  direction continua<sup>17</sup> and the characteristic asymmetric Fano line shape can clearly be seen in the  $\sigma^-$  spectrum.

For weak electric fields,  $F=10$  kV/cm, we observe discrete lines for excited states as clearly seen in the  $\sigma^+$  spectrum. The structure of the spectra is very complicated due to the interference between different Landau and Wannier-Stark states and also because of the mixing of light and heavy holes.

For intermediate fields ( $F=20, \dots, 30$  kV/cm), the spectra become simpler, because only vertical transitions with the same Wannier-Stark index ( $\Delta m=0$ ) remain in the energy region of interest. At the same time, the line width increases, compared to the case of  $F=10$  kV/cm.

In the high-field limit ( $F \geq 40$  kV/cm), the excited Wannier-Stark states lose their identity and transform into a flat continuum with a small modulation of the absorption profile. The lowest peak can still be distinguished from the rest of the spectrum. Its line width is considerably larger than in the low-field limit. The evolution of the lowest resonance is similar to what is observed for bulk semiconductors in electric fields.<sup>18</sup>

As already mentioned, the evolution of the experimental absorption spectra is qualitatively similar to that deduced from the two-band model when Zener tunneling is included. The agreement between theory and experiment is better at high fields. In contrast, the calculation without Zener tunneling (Fig. 3 of Ref. 13, dashed line) gives a spectrum, which

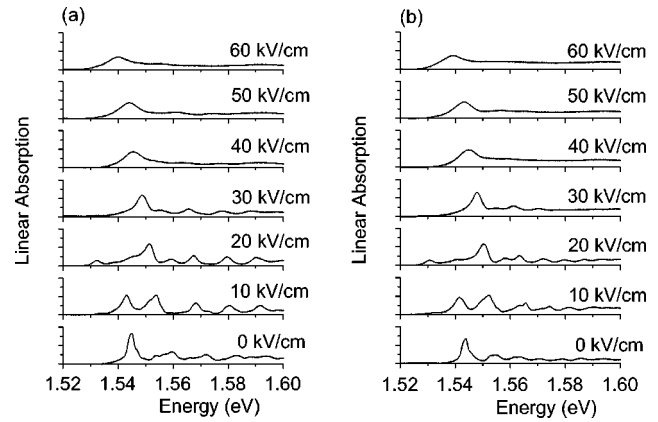


FIG. 4. Experimental absorption spectra for  $\sigma^-$  polarization and  $F=0, \dots, 60$  kV/cm. (a)  $B=6$  T. (b)  $B=4$  T.

is entirely discrete, in direct contradiction with the experiment.

For completeness, in Fig. 4 we show absorption spectra for  $\sigma^-$  polarization and lower magnetic fields,  $B=6$  T (a) and  $B=4$  T (b). The results only show some minor differences as compared to the high field,  $B=9$  T, case of Fig. 2. The absorption for  $F=10$  kV/cm no longer goes to zero between the resonances simply because the Landau level separation is now smaller. Furthermore, the onset of the Zener breakdown is shifted to lower electric fields, because the exciton binding energy, which increases with magnetic field, is reduced by the electric field.

In a recent paper, Bauer *et al.* studied photocurrent spectra of superlattices in Faraday geometry.<sup>19</sup> The fixed electric field was relatively small (10 kV/cm) and the superlattice was weakly coupled (17 Å barriers, Al content 30%), in comparison to our work. The spectra show distinct resonances the evolution of Landau fans with increasing magnetic field.

In order to make a comparison to Ref. 19, we present absorption spectra for several magnetic fields at fixed electric field. For the electric field, we choose a value below the

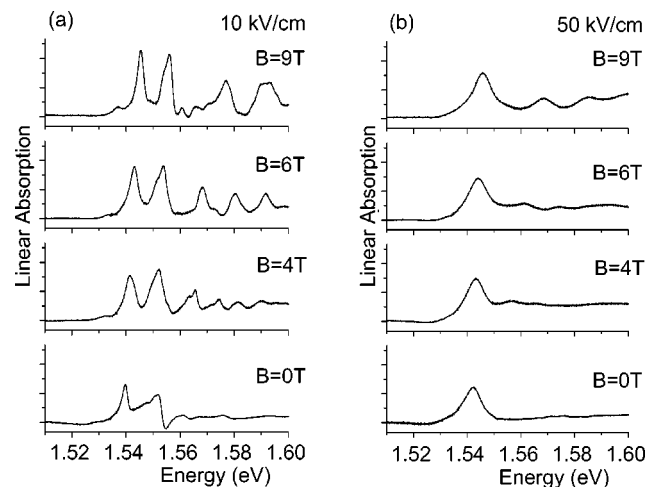


FIG. 5. Experimental absorption spectra for  $\sigma^-$  polarization and  $B=0, 4, 6,$  and  $9$  T. (a)  $F=10$  kV/cm. (b)  $F=50$  kV/cm.

Zener threshold,  $F = 10$  kV/cm, and above the Zener threshold,  $F = 50$  kV/cm. The results are shown in Fig. 5 (a) and (b). For small electric field (a), the spectrum is discrete at any magnetic field  $B \neq 0$ , in accordance with Ref. 19. The situation is very different in the high-field case (b). At  $B = 0$ , we observe a single line, which is strongly broadened, and a flat continuum. As  $B$  increases, no distinct lines emerge from the continuum. Only for large magnetic fields, when the cyclotron energy exceeds the Zener broadening, a small modulation of the continuum can be observed.

It is worthwhile to discuss the effects of homogeneous and inhomogeneous broadening on the results. In the absence of Zener tunneling, the optical transitions experience inhomogeneous and homogeneous broadening due to interface roughness and scattering. The exciton localization increases with magnetic field, because the extension of the exciton wave function in lateral direction is proportional to  $B^{-1/2}$ . At the same time the dimensionality of the semiconductor is reduced from 3 to 1, which means that the scattering is reduced. One can see this picture to be confirmed in Fig. 5(a). The broadening of the lowest resonance near 1.54 eV increases with magnetic field in the range  $B = 0, \dots, 4$  T. For

larger fields, the line narrows again. Thus we conclude that the line width at large magnetic field is mainly due to scattering. The line width at  $B = 9$  T (FWHM) is about 2.2 meV. In the calculations, which were made prior to the experiment, we used a Lorentzian line broadening of 2 meV.

In conclusion, our experimental results give clear evidence of Zener breakdown in superlattices with a perpendicular magnetic field, which directly manifests itself by the transition from discrete to continuous spectra in a true 1D system. The evolution of the absorption spectra with magnetic fields is in qualitative agreement with a two-band model when Zener tunneling is accounted for, but in complete contradiction when this effect is not included in the numerical calculations.

We acknowledge support by the Deutsche Forschungsgemeinschaft, contract No. LE 747/30, computing resources from the John von Neumann Center for Computing, Forschungszentrum Jülich. The work in Berkeley was supported by the Director, Office of Science, Office of Basic Energy Science, Division of Material Sciences and Office of Science, U.S. Department of Energy under contract No. DE-AC03-76SF00098.

- 
- <sup>1</sup>L. Esaki and R. Tsu, IBM J. Res. Dev. **61**, 61 (1970).  
<sup>2</sup>E.E. Mendez, A. Agulló-Rueda, and J.M. Hong, Phys. Rev. Lett. **60**, 2426 (1988).  
<sup>3</sup>P. Voisin, J. Bleuse, C. Bouche, S. Gaillard, C. Alibert, and A. Regreny, Phys. Rev. Lett. **61**, 1639 (1988).  
<sup>4</sup>K. Leo, P. Haring Bolivar, F. Brüggemann, R. Schwedler, and K. Köhler, Solid State Commun. **84**, 943 (1992).  
<sup>5</sup>H.M. James, Phys. Rev. **76**, 1611 (1949).  
<sup>6</sup>G.H. Wannier, Phys. Rev. **117**, 432 (1960).  
<sup>7</sup>G. Nenciu, Rev. Mod. Phys. **63**, 91 (1991).  
<sup>8</sup>J.E. Avron, J. Zak, A. Grossmann, and L. Gunther, J. Math. Phys. **18**, 918 (1977).  
<sup>9</sup>M. Ritze, N.J.M. Horing, and R. Enderlein, Phys. Rev. B **47**, 10 437 (1993).  
<sup>10</sup>S. Glutsch and F. Bechstedt, Phys. Rev. B **57**, 11 887 (1998).  
<sup>11</sup>C. Zener, Proc. R. Soc. London **145**, 523 (1934).  
<sup>12</sup>B. Rosam, D. Meinhold, F. Löser, V.G. Lyssenko, S. Glutsch, F. Bechstedt, F. Rossi, K. Köhler, and K. Leo, Phys. Rev. Lett. **86**, 1307 (2001).  
<sup>13</sup>S. Glutsch, F. Bechstedt, B. Rosam, and K. Leo, Phys. Rev. B **63**, 085307 (2001).  
<sup>14</sup>S. Glutsch and F. Bechstedt, Phys. Rev. B **60**, 16 584 (1999).  
<sup>15</sup>U. Rössler, Solid State Commun. **65**, 1279 (1988).  
<sup>16</sup>H. Chu and Y.C. Chang, Phys. Rev. B **40**, 5497 (1989).  
<sup>17</sup>S. Glutsch, U. Siegner, M.-A. Mycek, and D.S. Chemla, Phys. Rev. B **50**, 17 009 (1994).  
<sup>18</sup>D.F. Blossey, Phys. Rev. B **3**, 1382 (1971).  
<sup>19</sup>T. Bauer, A.B. Hummel, H. Roskos, and K. Köhler, Physica E (Amsterdam) **7**, 289 (2000).